

Antimicrobial effect of silver and gold nanoparticles in combination with linezolid on *Enterococcus* biofilm

Niloofar Sabzi¹, Rezvan Moniri¹, Mojtaba Sehat², Hadis Fathizadeh^{3,4}, Ali Nazari-Alam^{1,5*}

¹Department of Microbiology, Faculty of Medicine, Kashan University of Medical Sciences, Kashan, Iran

²Trauma Research Center, Kashan University of Medical Sciences, Kashan, Iran

³Student Research Committee, Sirjan School of Medical Sciences, Sirjan, Iran

⁴Department of Laboratory Sciences, Sirjan School of Medical Sciences, Sirjan, Iran

⁵Infectious Diseases Research Center, Kashan University of Medical Sciences, Kashan, Iran

Received: July 2022, Accepted: October 2022

ABSTRACT

Background and Objectives: In the past few years, application of new antimicrobial e.g. nanoparticles (NPs) to treat infection caused by drug-resistant bacteria has increased. This study aimed to determine antimicrobial property of silver nanoparticles (AgNPs) and gold nanoparticles (AuNPs) in combination with linezolid on *Enterococcus* biofilm.

Materials and Methods: A total of forty-eight isolates of *Enterococcus* spp. were collected and confirmed by PCR method. The synthesis of biocompatible AgNPs was performed, then analyzed by Fourier Transform Infrared spectroscopy (FTIR), Scanning Electron Microscopy (SEM), and Transmission Electron Microscopy. We carried out minimum inhibitory concentration (MIC) and biofilm forming capacity of AgNPs and AuNPs with linezolid.

Results: Twenty-two *E. faecium* isolates and twenty- six *E. faecalis* investigated in this study. Strong biofilm formation was seen in 12 (25%) of isolates, and others isolates (75%) formed moderate biofilm. AgNPs and Au-NPs size were 26 nm and 20 nm respectively. The MIC of AgNPs was 23.2 µg/ml, and AuNPs were 92.1 µg/ml and the lowest MIC was obtained 2 µg/ml in linezolid. Biofilm formation inhibitory activity by AuNPs + Linezolid and AgNPs + Linezolid 70 to 80 percent increased in average.

Conclusion: The antibiofilm activity of AgNPs and AuNPs increased when both agents were used in combination with linezolid in comparison with each agent alone.

Keywords: *Enterococcus faecalis*; *Enterococcus faecium*; Nanoparticles; Anti-bacterial agents; Biofilm

INTRODUCTION

The enterococci are important causes of nosocomial infections, chiefly in intensive care units, and are chosen by therapy with cephalosporins

and other antibiotics to which they are resistant (1). The most important pathogenic enterococci in humans contain *Enterococcus faecium* and *Enterococcus faecium*. *E. faecium* is usually much more antibiotic-resistant than *E. faecalis* (2). Owing

*Corresponding author: Ali Nazari-Alam, Ph.D, Department of Microbiology, Faculty of Medicine, Kashan University of Medical Sciences, Kashan, Iran; Infectious Diseases Research Center, Kashan University of Medical Sciences, Kashan, Iran. Tel: +98-3155540021-25 Fax: +98-3155541112 Email: nazarialam-a@kaums.ac.ir

to the different antimicrobial resistance mechanisms, effective treatment of enterococcal infections is becoming increasingly difficult. Newer agents for example linezolid are used for the treatment of VRE infections. Linezolid is an oxazolidinone antibiotic that inhibits protein synthesis. Linezolid is the single antibiotic presently accepted by the US Food and Drug Administration, but resistance to it is on the rise (3). Resistance to linezolid selected *in vitro* and has also been observed in clinical settings (4). Recent developments in nanotechnology to engineer nanoparticles with desired physicochemical properties have been projected as a new line of defense against vancomycin resistance infections (5). New ways to biofilm growth inhibition, biofilm damage, or biofilm eradication have been proposed. Nanoparticles have shown effective antimicrobial activity against vancomycin-resistant enterococci (6). The utility of nanomaterials for the development of anti-biofilm agents is well documented (7). AuNPs and AgNPs are extensively used NPs and show strong biocide effects on a broad spectrum of bacterial pathogens (6, 7). Therefore, the synergistic result of AgNPs and AuNPs with other antimicrobial agents has gotten much attention. The trends in the epidemiology of enterococcal infections recommend that MDR isolates may become the most usual species isolated from hospitalized patients shortly. Thus, new therapeutic strategies focused on treating infections with these organisms are immediately required. One approach to fighting MDR infections is to combine two or more antimicrobial agents during a treatment regimen. This study aimed to evaluate the antimicrobial and anti-biofilm activity of silver and gold nanoparticles alone and in combination with linezolid against *E. faecalis* and *E. faecium* clinical isolates.

MATERIALS AND METHODS

Bacterial strains. The isolates applied in this study were isolated from hospitalized patients at Shahid Beheshti hospital in Kashan, Iran, between 2017 and 2018. A total 48 of *Enterococcus* spp. isolates collected from clinical samples (stool, urine, peritoneal fluid, and wound) of hospitalized patients. Isolates cultured on blood agar and MacConkey agar and incubated at 37°C for 24 hours. Positive isolates examined by Gram staining and standard biochemical tests such as catalase, PYR, and growing on media

containing 6.5% salt. All isolates tested in PCR assay to determine the presence of *ddlE1* and *ddlF1* genes, which is specific to *E. faecalis* and *E. faecium*. They were verified by blast analysis in the database (<http://www.ncbi.nlm.nih.gov/GenBank>).

Primer pairs used for *ddlE1* gene with 941 base pair chain indicated as follows: Forward: 5'- ATCAAGTACAGTTAGTCTTTATTAG-3', and Reverse: 5'- AC-GATTCAAAGCTAACTGAATCAGT -3' for *E. faecalis* isolates and *ddlF1* gene with 658 base pair chain shown as follows: Forward: 5'- TTGAGGCAGAC-CAGATTGACG -3', and Reverse: 5'- TATGACAGC-GACTCCGATTCC -3' for *E. faecium* isolates.

Biofilm formation was examined as explained before (8). The exclusion criteria of the study also included enterococci clinical isolates that had a weak ability or no ability to form a biofilm.

Biosynthesis of nanoparticles. Au NPs were purchased from Nanomabna Company, Iran. The company produced these materials based on Turkevich Method. For the production of silver nanoparticles, 0.068 mM of silver nitrate was weighed and poured into 400 mL of sterilized distilled water, and it was dissolved. Then, 5 mL of Luria-Bertani medium (LB) was added to it. The solution was placed in an incubator (First, 24 hours, then, 48 hours, and finally, 72 hours). Then, it washed three times with water and twice with 96% alcohol. The supernatant discarded to dispose of any uncoordinated material. The solution washed thrice with distilled water to remove the remaining proteins or enzymes in the samples. Then it centrifuged and washed with alcohol; next, it centrifuged twice at 10,000 rpm for 20 minutes. After sonication, it dried with a vacuum drier for an overnight at 50°C (9).

UV-Visible absorbance spectroscopy. Bioreduction of Ag⁺ ions in AgNO₃ solution seen with ultraviolet-visible (UV-Vis) spectroscopy (UV-2800, BMS). The UV spectrums for 250, 350, 450, 550, 650 μL concentrations of the AgNO₃ solution was monitored. The UV-Vis absorption spectra for AgNPs were observed in a range of 300-800 nm with a UV-2800 spectrophotometer.

Fourier transforms infrared spectroscopy. Fourier transforms infrared (FTIR) spectroscopy method applied for the study of functional groups, chemical bonding of inorganic and organic samples, and mo-

lecular structure via producing an infrared absorption spectrum (Bruker Tensor 27, Germany).

X-ray diffraction. The crystalline nature and structural categorization of AgNPs were determined through an X-ray diffractometer for the vacuumed dried AgNPs.

Scanning electron microscopy. The morphology and size of AgNPs were examined by the JEOL-6490A-JSM scanning electron microscope (SEM). The elemental composition of AgNPs was determined with energy dispersive spectroscopy (TESCAN MIRA3).

Determination of MIC. Antimicrobial activity of the Ag-nanoparticle and Au-nanoparticle was determined by the broth microdilution method. Nanoparticles at the concentration of 742.5 µg/ml were serially (2-fold) diluted Mueller Hinton broth followed by the addition of each bacterial lane in their respective wells at 5×10^5 CFU/mL. Each lane was added with vehicle control (1% DMSO), positive control, and negative controls. Minimum inhibitory concentration (MIC) was noticed after incubation for 24 hours at 37°C. The lowest concentration of agent which prevented the growth has measured the MIC. After incubation OD was noted at 600 nm. From the graph, minimum inhibitory concentration and amount of inhibition at each concentration were calculated (10).

Biofilm activity. The microbial isolates were grown in Luria Broth (LB) (Merck, Germany) and then maintained for 18 until 24 hours at 37°C. The grown bacterial suspension was diluted to 1:100 in LB medium, and 200 µl of this cell suspension was applied to inoculate sterile flat-bottomed 96-well polystyrene microtiter plates (BD Biosciences). After 24 h at 37°C, wells were mildly washed three times with 300 µl of distilled water, dried in an inverted position, and stained with 300 µl of 2% crystal violet solution in water for 45 min. After staining, plates washed three times with distilled water. Quantitative analysis of biofilm formation done by adding 300 µl of ethanol-acetic acid (95:5, Vol/ Vol) to destain the wells. Finally, 100 µl from each well was transported to a new polystyrene microtiter plate, and the level (optical density; OD) of crystal violet was measured at 570 nm using an ELIZA plate reader. Each assay performed in triplicate. As a control, the un-inoculated

medium was used to determine background OD. The mean OD570 value from the control wells was subtracted from the mean OD570 value of tested wells. According to OD, the isolated bacteria were classified into three groups of strong OD $570 \geq 0.70$, moderate $0.38 < OD 570 < 0.70$, and OD570 ≤ 0.38 weak biofilm formers (10).

Antibiofilm activity. The anti-biofilm activity determined using the microtiter plate method. For this, *Enterococcus* inoculated in sterile tryptic soy broth and incubated for 24 h at 37°C. Then samples centrifuged at 5000 rpm, and the pellet suspended in phosphate buffer (pH 7.0) 1mg/ml stock of all nanoparticles prepared. Briefly, 200 µl medium with 1/2MIC, MIC, 2×MIC concentrations of nanoparticles inoculated with 10 µl of bacterial suspension to 5×10^5 CFU/ml concentration and incubated for 24h at 37°C. After incubation, the wells drained, washed with phosphate buffer saline (PBS), fixed with cold methanol, and then stained with 1% crystal violet for 30 min. The intensity of suspension measured at 570 nm, and percent of biofilm inhibition calculated using the equation given below (10).

Percentage of biofilm inhibition = $(OD 570 \text{ control} - OD 570 \text{ treatment} / OD570 \text{ control}) * 100$

Synergy testing

Fractional inhibitory concentration (FIC). The antimicrobial synergy effect of linezolid-AgNPs and linezolid-AuNPs was assessed by the same technique. Briefly, FIC to AgNPs, AuNPs, and linezolid antibiotics and synergism between them were tested using checkerboard microtiter plate assay (11). The minimum concentration of each of the mentioned antimicrobial substances that inhibited the growth of the indicator organism after 18 hours of incubation at 37°C was known as the MIC of each of the antimicrobial substances. The MIC of each nanoparticles or antibiotic were obtained and two higher (2×MIC) and two lower concentrations (1/2MIC) were investigated. To assess the result of the combination, the fractional inhibitory concentration (FIC) calculated for each antibiotic in each combination like this: FIC index = FIC of drug A + FIC of drug B; where FIC of drug A = MIC of drug A in combination / MIC of drug A alone; and FIC of drug B = MIC of drug B in combination / MIC of drug B alone. The results were interpreted as synergism if the FIC index ≤ 0.5 ; additive effect if the FIC

index of >0.5 and ≤ 4 ; and antagonism if the FIC index >4 . The procedure was replicated three times (11).

Statistical analysis. Data were analyzed in spss16. Statistical analyses performed based on Kolmogorov-Smirnov, Kruskal-Wallis, and Mann-Whitney tests.

RESULTS

Bacterial strains and biofilm activity. Among all *Enterococcus* isolates collected, only strong and moderate biofilm producing isolates, which included forty-eight isolates, were examined in this study. Other isolates were excluded from the study. Out of these bacterial isolates, 27 (56.3%) were prepared from feces, 15 (31.3%) were prepared from a urine culture, and other isolates were prepared from ulcer, tissue, and peritoneum.

Twenty-two *E. faecium* isolates and twenty-six *E. faecalis* included in this study. Strong biofilm was seen in 12 (25%) of isolates, and others formed moderate biofilm.

Biosynthesis of nanoparticles AgNPs

UV-vis. Spectroscopic analysis of silver nanoparticles synthesized with Luria Bertani Broth (LB) microbial culture medium with a spectrophotometer (UV-vis) and determining the maximum optical absorption at a wavelength of 420 nm in the wavelength range of 300 to 800 nm, which confirms the synthesis and creation of nanoparticles silver in small size (Fig. 1).

FTIR. Infrared spectroscopy (FTIR) analysis of silver nanoparticles produced using brain heart infusion broth culture medium showed the presence of absorption bands in the range of 1540-1640/cm, which indicates that the reduction and stability factor of silver nanoparticles is protein (Fig. 2).

XRD. The X-ray diffraction (XRD) diagram of the synthesized silver nanoparticles, based on the specified positions, which include 27.8630, 32.2796, 35.13, 38.15, 46.2724, 54.861, 64.58, 57.51, 74.491, 76.771, 77.47, the existence of silver nanoparticles has been confirmed (Fig. 3).

EDX. X-ray Energy Diffraction Spectroscopy (EDX) diagram of silver nanoparticles shows the elements

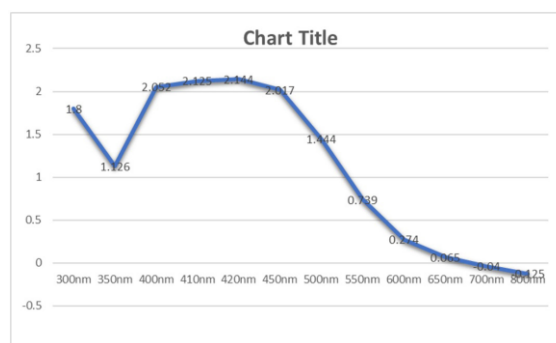


Fig. 1. Spectroscopic analysis of AgNPs synthesized with Luria Bertani Broth (LB) microbial culture medium with UV-vis and determining the maximum optical absorption at a wavelength of 420 nm in the wavelength range of 300 to 800 nm.

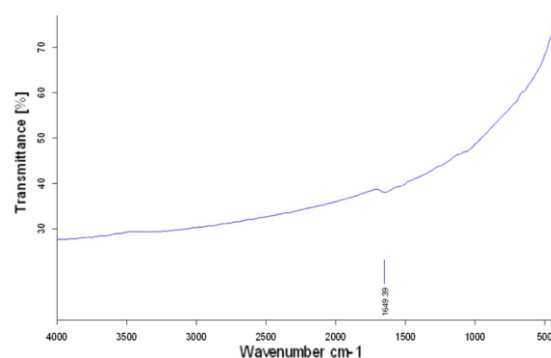


Fig. 2. FTIR analysis of AgNPs produced using brain heart infusion broth culture medium showed the presence of absorption bands in the range of 1540-1640/cm, which indicates that the reduction and stability factor of silver nanoparticles is protein.

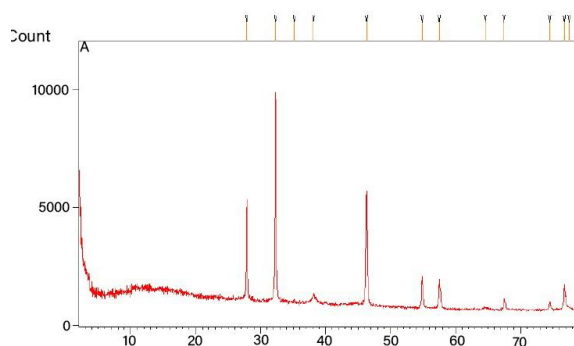


Fig. 3. The X-ray diffraction (XRD) diagram of the synthesized silver nanoparticles, based on the specified positions, which include 27.8630, 32.2796, 35.13, 38.15, 46.2724, 54.861, 64.58, 57.51, 74.491, 76.771, 77.47, the existence of silver nanoparticles has been confirmed.

present in the production sample, which includes silver at the rate of 78.5% and carbon and chlorine elements at a lower percentage (Fig. 4).

SEM. The scanning electron microscope (SEM) of the synthesized silver nanoparticles at the scale of 200 nm determines the square shape and size of the synthesized silver nanoparticles. The size of nanoparticles was between 20 and 100 nm (Fig. 5).

Biosynthesis of nanoparticles AuNPs

UV-vis. Spectroscopic analysis of gold nanoparticles with a spectrophotometer (UV-vis) and determining the maximum optical absorption at a wavelength of 521 nm in the wavelength range of 400 to 1000 nm, which is a confirmation of the synthesis and creation of gold particles (Fig. 6).

FTIR. Infrared spectroscopy (FTIR) analysis of produced gold nanoparticles, the presence of absorption bands in the range of 1540-1640, >3000/cm. It represents the functional group N-H, primary and secondary amine, and the range of 540-760/cm represents the functional group C-X related to chloroalkanes. These functional groups were agents for reduction and synthesis of gold nanoparticles (Fig. 7).

EDX. X-ray Energy Diffraction Spectroscopy (EDX) graph of gold nanoparticles shows the elements in the production sample which contains gold in the amount of 76.3% (Fig. 8).

SEM. Scanning Electron Microscope (SEM) of synthesized gold nanoparticles on a scale of 200 nm determines the shape and size of synthesized gold nanoparticles (Fig. 9).

Determination of MIC. The MIC values of AuNPs group was $92.19 \mu\text{g/ml} \pm 31.86$ (Minimum 75, Maximum 150); followed by the Ag-NPs group with $23.17 \mu\text{g/ml} \pm 4.48$ (Minimum 12, Maximum 25), and the lowest MIC was obtained $2 \mu\text{g/ml}$ in linezolid. The difference between groups was significant ($p < 0.001$) (Chart 1). The MIC₉₀ values AgNPs and AuNPs of *Enterococcus* isolates were 23.17 and $92.19 \mu\text{g/ml}$ respectively. The percentage of biofilm inhibition compared in all groups by level of concentration as shown in Table 1. In low (1/2MIC), optimum (MIC), and high dose (2×MIC) concentrations, the most percent-

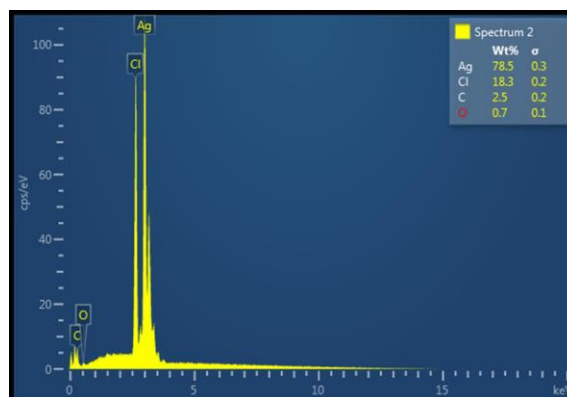


Fig. 4. EDX diagram of silver nanoparticles shows the elements present in the production sample, which includes silver at the rate of 78.5% and carbon and chlorine elements at a lower percentage.

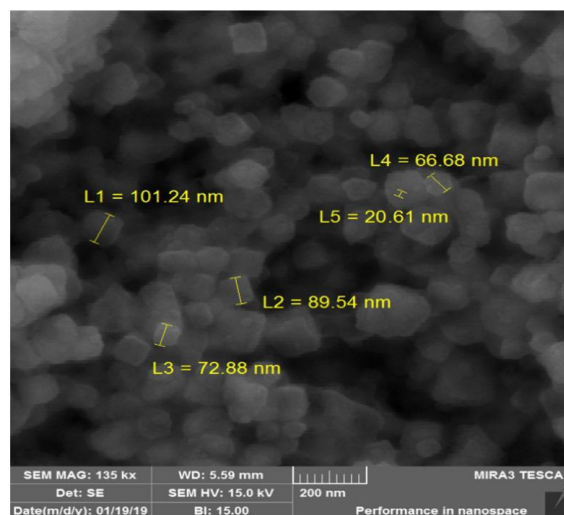


Fig. 5. Scanning electron micrographs (SEM) of AgNPs by TESCAN MIRA3, The size of nanoparticles (L1-L5) were between 20 and 100 nm.

age of inhibition were seen in AgNPs-linezolid and AuNPs-linezolid; while the difference between combination therapies was significant with single therapy in all doses. The P-value of the difference in high and lower dose was 0.001 and 0.005, respectively. Pair-wise comparison of the study groups in terms of biofilm inhibition in single therapy showed no significant difference between AgNPs and AuNPs in all doses.

Anti-biofilm activity and Synergy testing. The percentage of biofilm inhibition is shown in Chart 2. The rate of the combined effect of AuNPs-linezolid was compared with AgNPs-linezolid, as shown in

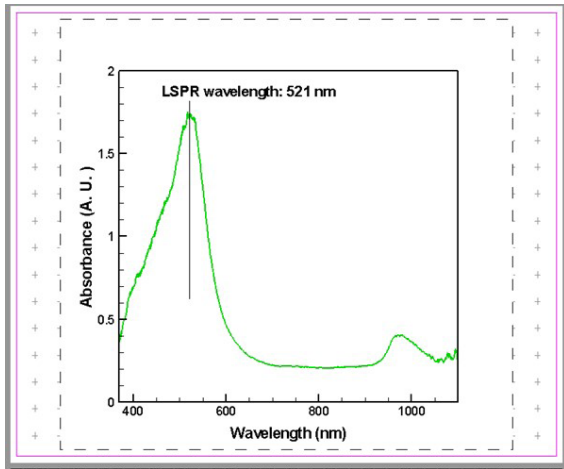


Fig. 6. UV-vis of AuNPs that determining the maximum optical absorption at a wavelength of 521 nm in the wavelength range of 400 to 1000 nm, which is a confirmation of the synthesis and creation of gold particle.

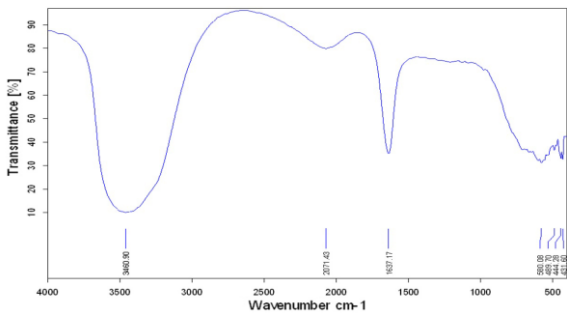


Fig. 7. FTIR analysis of produced gold nanoparticles, the presence of absorption bands in the range of 1540-1640, >3000/cm. It represents the functional group N-H, primary and secondary amine, and the range of 540-760/cm represents the functional group C-X related to chloroalkanes.

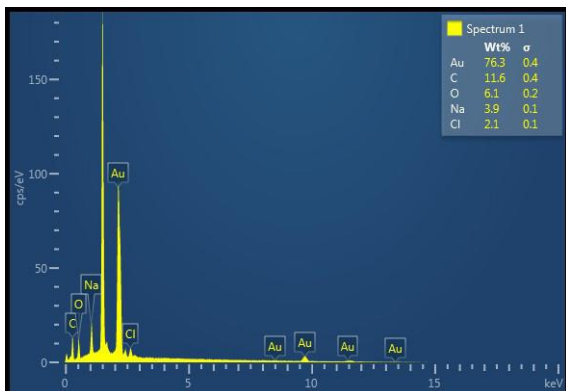


Fig. 8. EDX graph of gold nanoparticles shows the elements in the production sample which contains gold in the amount of 76.3%.

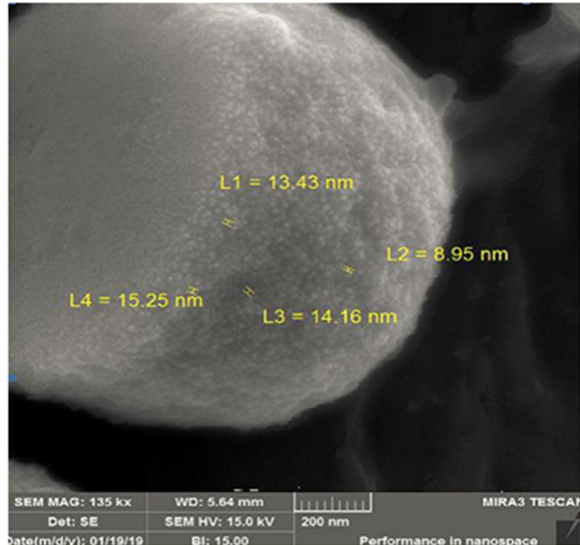


Fig. 9. Scanning electron micrographs (SEM) of AuNPs, The size of nanoparticles were between 8 and 15 nm.

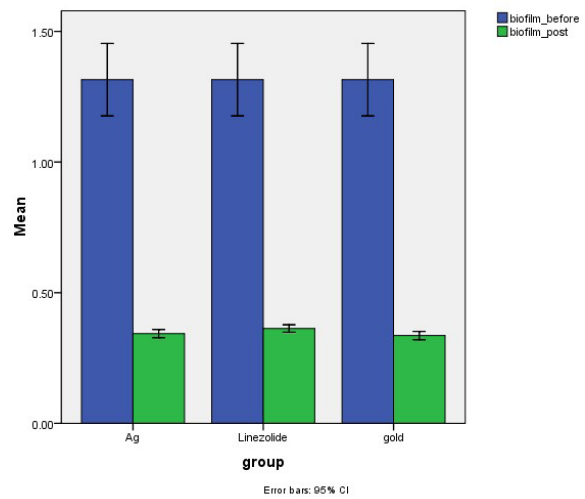


Chart 1. The level of biofilm changes before and after the intervention

Table 2, in the optimum and low concentrations; the difference between the two groups was significant in term of FBIC. However, it is not significant at high concentrations. Synergism effect in three concentrations (1/2MIC, MIC, and 2×MIC) compared between two combination groups of AgNPs-linezolid, and AuNPs-linezolid shown in Chart 3. It is shown that AgNPs-linezolid had a more synergistic effect than AuNPs-linezolid in all concentrations, but except for a high concentration group, the difference was not significant in other concentrations ($p=0.028$). The outcome of combinational antibiofilm activities of AgNPs and AuNPs with linezolid described in Table 3. On aver-

Table 1. MIC distribution in three studied groups

P value	Groups			Average	Standard Deviation	MIC ($\mu\text{g/ml}$)
	AuNPs	Linezolid	AgNPs			
<0.001	92.19	2	23.17			
	31.86	0	4.48			
	75	2	12	Least		
	150	2	25	Most		
	75	2	25	Middle		
	75	2	25	Mode		

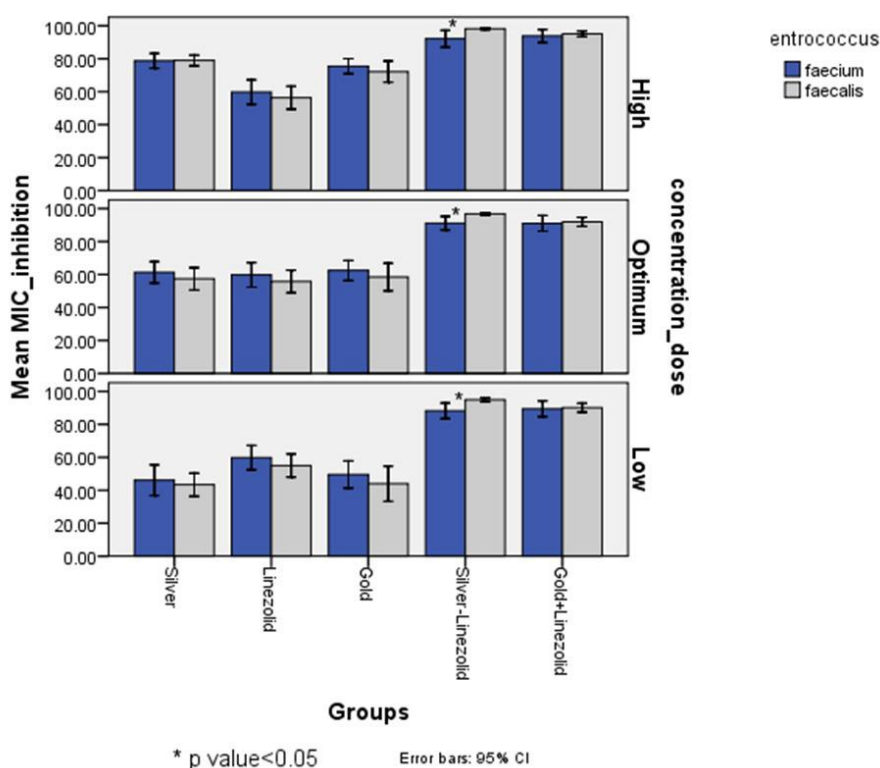


Chart 2. Comparison of percent of biofilm inhibition between *E. faecium* and *E. faecalis* in five study groups by level of concentration (Linezolid, AgNPs, AuNPs, Linezolid+AgNPs, Linezolid+AuNPs). High: 2×MIC; Optimum: MIC; Low: 1/2MIC

age, 69 to 83% of *Enterococcus* isolates had synergistic properties in all three mentioned concentrations (1/2MIC, MIC, and 2×MIC) in the combination of nanoparticles with linezolid. However, combination of AgNPs-linezolid had a more synergic effect than the combination of AuNPs-linezolid in all concentrations in *E. faecalis* significantly, while the difference in *E. faecium* was not significant. A comparison of FBIC at different levels is shown in Table 4. Therefore, it is identified that the difference between the two groups (AgNPs-linezolid and AuNPs-linezolid) in MIC and 1/2 MIC concentration is significant based of FBIC, but

the difference between the two groups is not significant at the FBIC 2×MIC level.

DISCUSSION

For the synthesis of AgNPs, Luria Bertani medium was used. It is considered as a new method to date (9). The advantage of this synthesis method over the chemical and physical method is the production and stability of silver nanoparticles in one step, low toxicity, and saving in time and cost. The size and surface

Table 2. percentage of biofilm inhibition compared in all groups by level of concentration

Groups	Low Concentration Inhibition (1/2MIC) Mean (SD)	Optimum Concentration Inhibition (MIC) Mean (SD)	High Concentration Inhibition (2×MIC) Mean (SD)
Silver	44.66 (18.93)	59.19 (15.79)	78.87 (8.96)
Linezolid	57.18 (17.05)	57.62 (16.78)	57.92 (16.90)
Gold	46.55 (23.12)	60.31 (17.79)	73.70 (13.59)
Silver-linezolid	91.86 (8.05)	94.18 (7.02)	95.41 (8.36)
Gold-linezolid	89.78 (8.65)	91.56 (8.69)	94.53 (6.68)
P value*	<0.001	<0.001	<0.001

* Kruskal Wallis Test

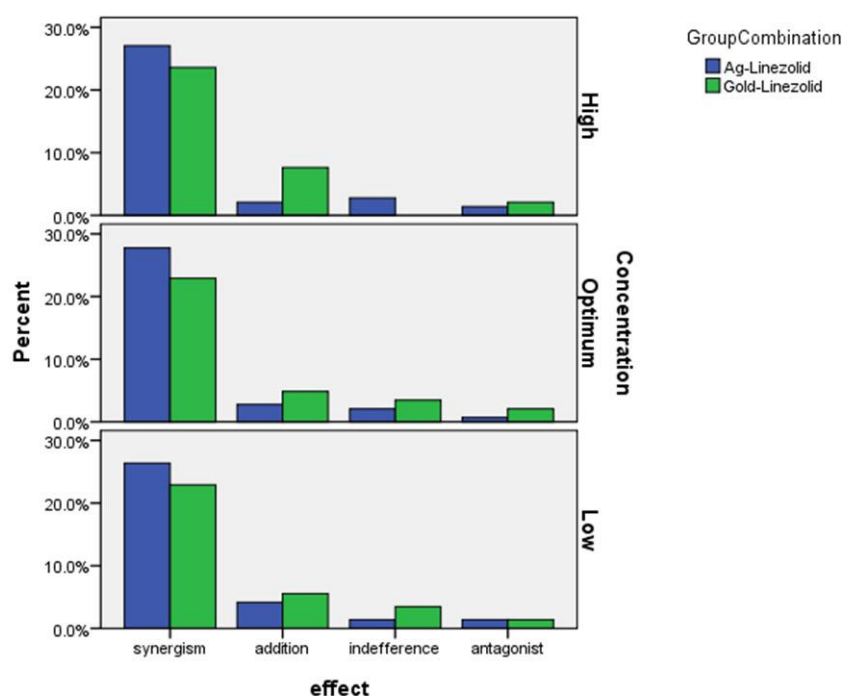


Chart 3. Comparison of the synergism effect of Linezolid + AgNPs and Linezolid + AuNPs in *Enterococcus* isolates at optimum, high and low concentrations

High: 2×MIC; Optimum: MIC; Low: 1/2MIC

coating of silver nanoparticles has an important role in antibacterial activity. AuNPs show antibacterial effect by making a change in membrane potential, inhibiting ATPase, and preventing the subunit of the ribosome for tRNA (12). AuNPs have been considered in biotechnology owing to their unique properties and multifunctional surface. This multidimensional surface is used to bind oligonucleotides, antibiotics, and proteins (12, 13). The antibacterial properties of gold nanoparticles showed that spherical gold nanoparticles with a maximum optical density of 534 nm and a

mean size 17 to 11 nm had a good antibacterial activity against Gram-positive bacteria (12). In this study, it was shown that the FBIC level was significantly different in the two combined groups at basic (MIC) and low concentrations (1/2 MIC). These results are consistent with the study conducted by Salunke et al. in 2014 in confirming the inhibition of planktonic bacterial growth and reduction of biofilm level (14). Treatment with the gold nanoparticles covered with indolicidin (AuNPs-indolicidin), considerably prevents the ability of *C. albicans* to form biofilms and

Table 3. The outcome of combinational anti-biofilm activities of AgNPs and AuNPs with Linezolid

Group	Outcome	AgNPs + linezolid	AuNPs + Linezolid
		No. (%)	No. (%)
2×MIC	Synergism	39 (81.3)	34 (70.8)
	Additive	3 (6.3)	11 (22.9)
	Indifference	4 (8.3)	0 (0)
	Antagonism	2 (4.2)	3 (6.3)
MIC	Synergism	40 (83.3)	33 (68.8)
	Additive	4 (8.3)	7 (14.8)
	Indifference	3 (6.3)	5 (10.4)
	Antagonism	1 (2.1)	3 (6.3)
1/2MIC	Synergism	38 (79.2)	33 (68.8)
	Additive	6 (12.5)	8 (16.7)
	Indifference	2 (4.2)	5 (10.4)
	Antagonism	2 (4.2)	2 (4.2)

Synergism: FIC index ≤ 0.5 ; additive effect: FIC index of >0.5 and ≤ 4 ; FIC index of 1–2: indifference; antagonism: FIC index >4 .

Table 4. Comparison of FBIC at different levels in combined study groups

FBIC Concentration	Ag NPs+Linezolid Mean (SD)	Au NPs+Linezolid Mean (SD)	P value*
High (2×MIC)	0.41 (0.80)	0.46 (0.73)	0.122
Optimum (MIC)	0.32 (0.44)	0.53 (0.46)	0.007
Low (1/2 MIC)	0.38 (0.47)	0.53 (0.58)	0.006

*Mann-Whitney Test

damages mature biofilms (15). The synergism effects of gold nanoparticles with antibiotics were similar to other studies. Vijayakumar et al. described that the gold nanoparticles synthesized using *Musa paradisica* peel extract (MPPE-AuNPs) effectively inhibited the biofilm of *E. faecalis* when experienced at $100\text{-}\mu\text{g mL}^{-1}$ (16). Synergistic interactions observed when combinations of AgNPs and the conventional antibiotics tested against isolates of methicillin-resistant *Staphylococcus aureus* (17). Combination therapy can be used to combat serious infections caused by multidrug-resistant bacteria. Katva et al. described that the combination of AgNPs with chloramphenicol and gentamicin has an enhanced antibacterial effect, and the combined effect of AgNPs with antibiotics was more as compared to AgNPs alone, which signify the synergistic effect of these nanoparticles (18). The antibacterial activity of AgNPs was

induced by ATP-related metabolism rather than by the permeability of the outer membrane. Moreover, AgNPs produced hydroxyl radicals, a highly reactive oxygen species made by bactericidal agents. AgNPs have likely as a combination therapeutic agent for the management of infectious diseases (19–23). Linezolid combination therapy may be a suitable method to improve effectiveness and prevent the development of resistance of vancomycin-resistant *E. faecium* (24). Treatment for enterococcal infections is complex by the fact that strains show inherent resistance to too many usually applied agents (23). As well, enterococci have obtained resistance to an extensive kind of antibiotic classes. The collective use of antibiotics with nanoparticles appears to be the most hopeful therapeutic choice for bacterial biofilm. Consistent with our study, the combination of AgNPs with linezolid could be a successful solution to decrease biofilm at lesser and fewer toxic doses. This study defines the antibacterial and anti-biofilm efficacy of the AgNPs synthesized by the LB medium. The most important advantages of this technique in excess of chemical procedures is little harmfulness and shorter manufacturing period and it is more affordable, as well as, nanoparticles that are created *in vitro*, physically affinity to be agglomerate; So it is necessary to stabilize these materials, but, with this present method, procedures and stability done simultaneously by LB medium. AgNPs prepared exhibited effective inhibition of biofilm formation. The inhibitory effect

of silver nanoparticles on the growth of enterococci biofilm was greater than gold nanoparticles, and this issue was observed at low concentrations.

CONCLUSION

As a result, it is better to use a silver nanoscale that is more cost-effective. The antibiofilm activity of AgNPs and AuNPs increased when both agents were used in combination with linezolid in comparison with each agent alone. These results suggest that the combination of AgNPs, AuNPs with linezolid can have clinical effects in the treatment of enterococcal infections. However, in vivo studies are needed before recommending the use of these nanoparticles in safety in clinical conditions.

REFERENCES

- García-Solache M, Rice LB. The *Enterococcus*: a model of adaptability to its environment. *Clin Microbiol Rev* 2019; 32(2): e00058-18.
- Jahansepar A, Ahangarzadeh Rezaee M, Hasani A, Sharifi Y, Rahnamaye Farzami M, Dolatyar A, et al. Molecular epidemiology of vancomycin-resistant *Enterococcus faecalis* and *Enterococcus faecium* isolated from clinical specimens in the Northwest of Iran. *Microb Drug Resist* 2018; 24: 1165-1173.
- Marshall S, Donskey CJ, Hutton-Thomas R, Salata RA, Rice LB. Gene dosage and linezolid resistance in *Enterococcus faecium* and *Enterococcus faecalis*. *Antimicrob Agents Chemother* 2002; 46: 3334-3336.
- Abbo L, Shukla BS, Giles A, Aragon L, Jimenez A, Camargo JF, et al. Linezolid-and vancomycin-resistant *Enterococcus faecium* in solid organ transplant recipients: infection control and antimicrobial stewardship using whole genome sequencing. *Clin Infect Dis* 2019; 69: 259-265.
- Lee N-Y, Ko W-C, Hsueh P-R. Nanoparticles in the treatment of infections caused by multidrug-resistant organisms. *Front Pharmacol* 2019; 10: 1153.
- Mulani MS, Kamble EE, Kumkar SN, Tawre MS, Pardesi KR. Emerging strategies to combat ESKAPE pathogens in the era of antimicrobial resistance: a review. *Front Microbiol* 2019; 10: 539.
- Pelgrift RY, Friedman AJ. Nanotechnology as a therapeutic tool to combat microbial resistance. *Adv Drug Deliv Rev* 2013; 65: 1803-1815.
- Moniri R, Ghasemi A, Moosavi SGA, Dastehgoli K, Rezaei M. Virulence gene's relationship with biofilm formation and detection of aac (6')/aph (2'') in *Enterococcus faecalis* isolated from patients with urinary tract infection. *Jundishapur J Microbiol* 2013; 6(5): e94137.
- Solouki M, Moniri R, Fathizadeh H, Kashi Jookar F, Moosavi GA, Nazari-Alam A. Green synthesis of silver nanoparticles using brain heart infusion (BHI) culture medium and evaluation of their antimicrobial and Anti-biofilm activity against *Acinetobacter baumannii*. *Mediterr J Infect Microbes Antimicrob* 2021; 10: 50.
- Fallah F, Yousefi M, Pourmand MR, Hashemi A, Nazari Alam A, Afshar D. Phenotypic and genotypic study of biofilm formation in *Enterococci* isolated from urinary tract infections. *Microb Pathog* 2017; 108: 85-90.
- Narasimhaswamy N, Bairy I, Shenoy G, Bairy L. In vitro activity of recombinant lysostaphin in combination with linezolid, vancomycin and oxacillin against methicillin-resistant *Staphylococcus aureus*. *Iran J Microbiol* 2017; 9: 208-212.
- Vimbela GV, Ngo SM, Frazee C, Yang L, Stout DA. Antibacterial properties and toxicity from metallic nanomaterials. *Int J Nanomedicine* 2017; 12: 3941-3965.
- Sarfraz N, Khan I. Plasmonic gold nanoparticles (AuNPs): properties, synthesis and their advanced energy, environmental and biomedical applications. *Chem Asian J* 2021; 16: 720-742.
- Salunke GR, Ghosh S, Santosh Kumar RJ, Khade S, Vashisth P, Kale T, et al. Rapid efficient synthesis and characterization of silver, gold, and bimetallic nanoparticles from the medicinal plant *Plumbago zeylanica* and their application in biofilm control. *Int J Nanomedicine* 2014; 9: 2635-2653.
- De Alteriis E, Maselli V, Falanga A, Galdiero S, Di Lella FM, Gesuele R, et al. Efficiency of gold nanoparticles coated with the antimicrobial peptide indolicidin against biofilm formation and development of *Candida* spp. clinical isolates. *Infect Drug Resist* 2018; 11: 915-925.
- Vijayakumar S, Vaseeharan B, Malaikozhundan B, Gopi N, Ekambaram P, Pachaiappan R, et al. Therapeutic effects of gold nanoparticles synthesized using *Musa paradisica* peel extract against multiple antibiotic resistant *Enterococcus faecalis* biofilms and human lung cancer cells (A549). *Microb Pathog* 2017; 102: 173-183.
- Akram FE, El-Tayeb T, Abou-Aisha K, El-Azizi M. A combination of silver nanoparticles and visible blue light enhances the antibacterial efficacy of ineffective antibiotics against methicillin-resistant *Staphylococcus aureus* (MRSA). *Ann Clin Microbiol Antimicrob* 2016; 15: 48.
- Katva S, Das S, Moti HS, Jyoti A, Kaushik S. Antibacterial synergy of silver nanoparticles with gentamicin and chloramphenicol against *Enterococcus faecalis*.

- Pharmacogn Mag* 2018; 13(Suppl 4): S828-S833.
19. Hwang I-S, Hwang JH, Choi H, Kim K-J, Lee DG. Synergistic effects between silver nanoparticles and antibiotics and the mechanisms involved. *J Med Microbiol* 2012; 61: 1719-1726.
 20. Wypij M, Świecimska M, Czarnecka J, Dahm H, Rai M, Golinska P. Antimicrobial and cytotoxic activity of silver nanoparticles synthesized from two haloalkaliphilic actinobacterial strains alone and in combination with antibiotics. *J Appl Microbiol* 2018; 124: 1411-1424.
 21. Wan G, Ruan L, Yin Y, Yang T, Ge M, Cheng X. Effects of silver nanoparticles in combination with antibiotics on the resistant bacteria *Acinetobacter baumannii*. *Int J Nanomedicine* 2016; 11: 3789-3800.
 22. Kamble SP, Shinde KD. Anti-biofilm activity against gram-positive bacteria by biologically synthesized silver nanoparticles using *Curcuma longa*. *Pharm Nanotechnol* 2018; 6: 165-170.
 23. Lopez-Carrizales M, Velasco KI, Castillo C, Flores A, Magaña M, Martinez-Castanon GA, et al. *In vitro* synergism of silver nanoparticles with antibiotics as an alternative treatment in multiresistant uropathogens. *Antibiotics (Basel)* 2018; 7: 50.
 24. Chen H, Du Y, Xia Q, Li Y, Song S, Huang X. Role of linezolid combination therapy for serious infections: review of the current evidence. *Eur J Clin Microbiol Infect Dis* 2020; 39: 1043-1052.